

On the Crystalline Structure of Even Polyoxalamides

Maria Teresa Casas, Elaine Armelin, Carlos Alemán, and Jordi Puiggali*

Departament d'Enginyeria Química, Universitat Politècnica de Catalunya, Av. Diagonal 647, E-08028, Barcelona, Spain

Received June 4, 2002; Revised Manuscript Received August 9, 2002

ABSTRACT: The crystalline structure of nylon 12 2 has been studied by means of X-ray and electron diffraction. Two structures can be obtained, depending on the preparation conditions. Both are based on a progressive stacking of hydrogen-bonded sheets, but they differ in the chain axis shift between consecutive sheets. Packing energy calculations corroborate these observations and indicate as the most stable a structure with only 1 Å shift. In the same way, theoretical calculations were also performed with nylon 6 2. Similarly, a structure with a different shift from the characteristic value of most conventional nylons is stabilized. Electron charge distributions on the oxalamide and amide groups play a fundamental role, thus favoring different stacking modes.

Introduction

Polyoxalamides ($-\text{[NH}(\text{CH}_2)_n\text{NHCOCO]}_x-$) can be considered as a peculiar class of nylons derived from diamines and dicarboxylic acids that has some peculiar properties due to the presence of stiff units, i.e., low solubility, high modulus, and high melting temperatures.^{1,2} Although the structure of aliphatic polyamides has been extensively studied,³ data on polyoxalamides are scarce. In this sense, analysis of fiber X-ray diffraction patterns of nylon 6 2⁴ points to a structure similar to the well-established α -form of nylon 6 6, which is based on a stacking of hydrogen-bonded sheets with a progressive shift along both the chain axis and the hydrogen-bonding directions.⁵ Nylon 9 2 has also been characterized by means of X-ray and electron diffraction, a structure with two hydrogen-bonding directions being postulated due to the presence of an odd diamine unit.^{6,7} Structural information is lacking for the rest of polyoxalamides, since only powder X-ray diffraction data have been reported for some even polyoxalamides, such as nylons 4 2, 8 2, 10 2, and 12 2.^{8,9} Strong reflections corresponding to spacings of about 4.5 and 3.7 Å have generally been observed together with a large spacing reflection associated with the chain repeat. This varies linearly from 10.8 Å in nylon 8 2 to 12.6 Å in nylon 10 2 to 14.5 Å in nylon 12 2 and contrasts with the low value of 6.4 Å observed in nylon 6 2. Therefore, these data suggest that the structure of even polyoxalamides depends on the length of their polymethylene segment, as is usual in even even nylons. In these polymers, a structure with a staggered shear along the chain axis direction between hydrogen-bonded sheets (named β -form) is stabilized when the number of methylene groups is large. In this paper, the structure of nylon 12 2 is reported and an energetic analysis is carried out with representative polymers of the series of even polyoxalamides.

Experimental Section

Nylon 12 2 was synthesized from 1,12-diaminododecane and diethyloxalate according to the two-step procedure reported by Shalaby et al.⁹ First, a prepolymer was obtained by reaction of the stoichiometric amounts of the monomers in a trifluoroethanol solution (20 min at room temperature, followed by 24 h at reflux). Second, a post-polycondensation was carried out in a vacuum at 250 °C for 6 h, and then at 270 °C for an

additional 5 h. The polymer was purified by precipitation with water from a dichloroacetic solution (1% w/v), and then successively washed with water, ethanol and ether.

An intrinsic viscosity of 0.84 dL/g was measured in dichloroacetic acid at 25 °C. A melting point of 232 °C was determined at a heating run of 20 °C/min with a Perkin-Elmer DSC-PYRIS 1 and using indium metal for calibration. Infrared absorption spectra were recorded from powder samples with a Perkin-Elmer 1600 FT-IR spectrometer in the 4000–500 cm^{-1} range. The main absorptions were: 3298 (amide A), 3049 (amide B), 2921 and 2850 (symmetric and asymmetric stretching of CH_2), 1649 (amide I), 1515 (amide II), 790 (amide V), and 536 cm^{-1} (amide VI). Density of fibers was determined in mixtures of ethanol and CCl_4 at 25 °C by the flotation method.

Isothermal crystallization was carried out at 165 °C from dilute solutions (0.005% w/v) in 2-methyl-2,4-pentanediol. The crystals were recovered from the mother liquor by centrifugation, repeatedly washed with *n*-butanol, and deposited on carbon-coated grids, which were shadowed with Pt-carbon at an angle of 15° for bright field observations. Polymer decoration was achieved by evaporating polyethylene on the surface of single crystals, as described by Wittmann and Lotz.¹⁰ A Philips TECNAI 10 electron microscope was used and operated at 80 and 100 kV for bright field and electron diffraction modes, respectively. Selected area electron diffraction patterns were recorded on Kodak Tri-X films. The patterns were internally calibrated with gold ($d_{111} = 0.235$ nm).

X-ray diagrams were recorded in a vacuum at room temperature, with calcite as a calibration standard. A modified Statton camera (W. R. Warhus, Wilmington, DE) with Ni-copper radiation of wavelength 0.1542 nm was used. Fibers were prepared from the melt and annealed under stress at 80 °C. Mats of sedimented crystals were prepared by slow filtration of a crystal suspension on a glass filter.

Structural modeling was carried out by using the software packages (diffraction and energy minimization) of the CERIUSt² (Biosym/Molecular Simulations Inc.)¹¹ and PCSP¹² (prediction of crystal structure of polymers) computer programs. Basically, in the energy minimization (CERIUSt² and PCSP), the relative stability of the different arrangements for a given packing was evaluated by varying the shift between consecutive hydrogen-bonded sheets. Energy contributions of both van der Waals and electrostatic interactions concerning closely spaced nonbonded atoms were taken into account. PCSP calculations were performed considering pseudoatoms for the methylene groups of the aliphatic segment, while all the atoms were explicitly defined in CERIUSt² minimizations. The values for the potential constants were taken from Dreiding¹³ (CERIUSt²) and Amber¹⁴ (PCSP) force-field libraries,

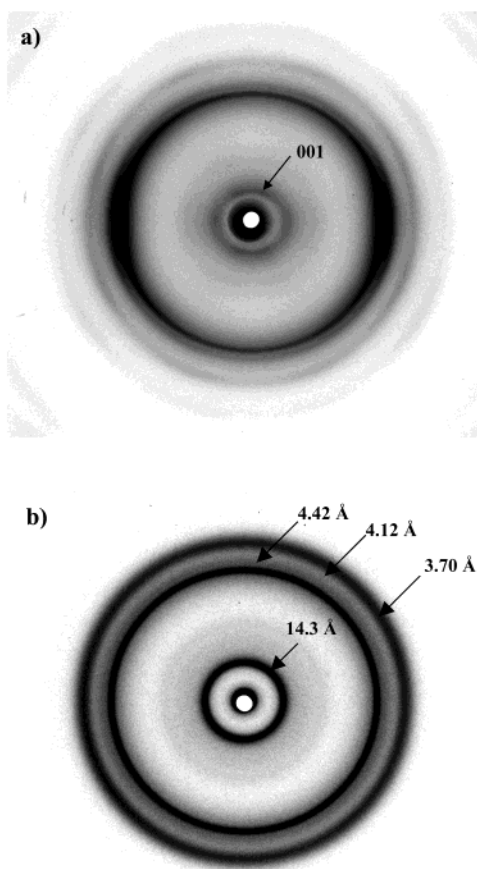


Figure 1. X-ray diffraction patterns corresponding to a fiber sample stretched from the melt (a) and a powder recovered directly from the polymerization medium (b). Note that the high spacing reflection observed in both patterns clearly changes (from 18 to 14.3 Å).

whereas the partial charges were explicitly derived from a representative small compound by using a well-established methodology.¹⁵ All calculations were run on a Silicon Graphics Indigo Workstation.

Results and Discussion

X-ray Diffraction. Figure 1a shows the X-ray diffraction pattern of a fiber obtained from the melt and annealed under stress at 100 °C. The most interesting feature is the presence of the 001 and 002 reflections, which define a cc^* angle close to 20°. This value is lower than the angle of 58° calculated from the reported cell dimensions of nylon 6 2 ($a = 5.15$ Å, $b = 7.54$ Å, and c (chain axis) = 12.39 Å and $\alpha = 32.4^\circ$, $\beta = 73.5^\circ$, and $\gamma = 61.9^\circ$) and may suggest a structure related to a conventional β form. However, it is significant that all reflections can be indexed by considering a triclinic unit cell (Table 1) with a b parameter close to 4 Å, which is the expected intersheet distance of a conventional α form. Note that a unit cell with a double value of this parameter is necessary to take into account the recuperative disposition of layers. It is also remarkable that the 01/ reflections (indexed according to the large unit cell) appear intense in the diffraction patterns of nylons with such a structure, and do not appear intense in the experimental fiber pattern of nylon 6 2.

Some parameters of the unit cell were chosen in order to optimize hydrogen-bonding geometry between neighboring chains. Thus, values of $4.79/\cos 78^\circ$ and 78°

Table 1. Measured and Calculated Spacings for Nylon 12 2 Fibers

| index | d_{calcd}^a (Å) | d_{meas}^b (Å) |
|--------------|--------------------------|-------------------------|
| 001 | 18.2 | 18.0 s off M |
| 002 | 9.1 | 9.10 w off M |
| 100 | 4.39 | 4.42 vs E |
| 10 $\bar{1}$ | 4.19 | 4.13 s E |
| 010 | 3.67 | }3.65 s E |
| 110 | 3.62 | |
| 01 $\bar{2}$ | 3.14 | 3.12 m off M |
| 007, 117 | 2.60, 2.52 | 2.65 w off M |
| 110 | 2.38 | }2.35 s E |
| 210 | 2.34 | |
| 018 | 2.20 | 2.21 m off M |
| 108 | 2.09 | 2.12 m off M |

^a On the basis of a triclinic unit cell with $a = 4.90$ Å, $b = 4.21$, $c = 19.2$ Å, $\alpha = 72^\circ$, $\beta = 78^\circ$, and $\gamma = 64^\circ$. ^b Abbreviations denote relative intensities or orientation: vs, very strong; s, strong; m, medium; w, weak; M, meridional; E, equatorial; off M, off meridional.

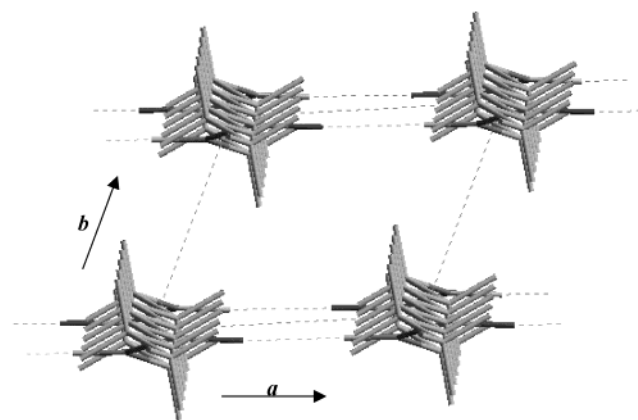


Figure 2. Down the chain axis projection of the nylon 6 2 unit cell. An angle of 66.4° defines the oblique unit cell, as usual in polyamides. Hydrogen bonds are established along the a crystallographic axis (dashed lines). Note that the oxalamide planes are slightly rotated from that defined by methylene carbons.

were selected for the a and β parameters of the unit cell, respectively. The other parameters were established in order to obtain the best agreement between calculated and experimental spacings. The final unit cell parameters were $a = 4.90$ Å, $b = 4.21$ Å, $c = 19.2$ Å, $\alpha = 72^\circ$, $\beta = 78^\circ$, and $\gamma = 64^\circ$. A theoretical density of 1.25 g/mL was calculated for a cell containing only one chain segment. This value was in good agreement with the experimental density of 1.22 g/mL, which was slightly lower due to the amorphous content of the sample. The deduced value of $\alpha = 72^\circ$ showed an interesting fact: neighboring sheets are shifted approximately 1 Å along the chain axis direction. This feature is peculiar in nylons, since a three bond shift (≈ 3.7 Å) is usually postulated taking into account both analysis of X-ray fiber diffraction patterns¹⁶ and crystallographic data on model compounds.¹⁷ Also note that the deduced c parameter (19.2 Å) is slightly shorter than the expected value for a fully extended conformation (19.6 Å). As usual in polyamides, the $\text{CH}_2\text{CH}_2\text{-NHCO}$ torsional angles may be stabilized in the $\pm 150\text{--}160^\circ$ range, yielding the indicated deviation from planarity¹⁸ (Figure 2). In this case, molecular symmetry is reduced to an inversion center placed in the middle of both diamine and oxaloyl units, a fact compatible with the expected $P\bar{1}$ space group for the postulated triclinic structure.

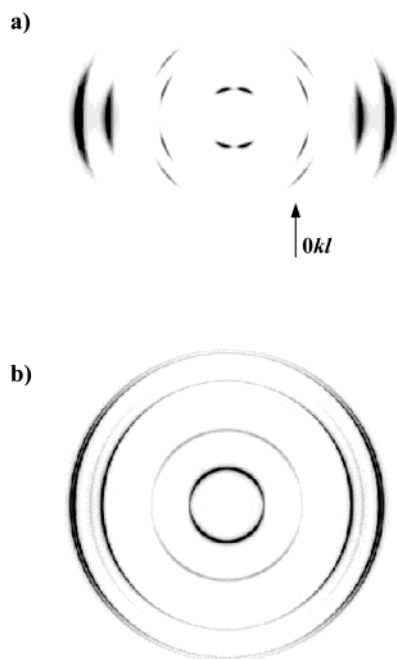


Figure 3. (a) Simulated fiber X-ray diffraction pattern corresponding to a hypothetical β structure with a staggered shear between hydrogen-bonded sheets of 3.6 Å along the chain axis direction. Note the intense 01/ reflections. (b) Simulated X-ray diffraction pattern corresponding to a conventional α -form with a 3.6 Å shift between consecutive hydrogen-bonded sheets.

The powder X-ray diffraction pattern of a sample coming directly from polymerization (Figure 1b) shows as the most intense the reflections observed at 4.42 and 3.70 Å, associated with the molecular packing, and at 14.3 Å. This value is intermediate between the spacings of 18.2 Å (001 reflection of the fiber diffraction pattern) and 10 Å (calculated value assuming the unit cell angles of nylon 6 2 and a chain repeat of 19.2 Å). The experimental repeats of 18.2 and 14.3 Å suggest that structures with a different sheet stacking could be stabilized depending on the sample preparation. In this sense, energy calculations show a not well-defined minimum energy packing, as will be explained.

X-ray diffraction patterns simulated with the CE-RIUS² program show the better agreement of progressive sheet structures with respect to a conventional and hypothetical β structure (Figure 3). This is based on a recuperative sheet displacement of 3.6 Å (Figure 4). Unit cell parameters of $a = 5.10$ Å, $b = 8$ Å, $c = 19.2$ Å, $\alpha = 90^\circ$, $\beta = 70^\circ$, and $\gamma = 68^\circ$ were selected in order to keep the experimental cc^* angle of the fiber pattern and an α angle of 90° , as is characteristic of a β form with a staggered sheet displacement. Note that in this case the β angle of 70° is not optimal for the establishment of hydrogen-bonding interactions, and that the a parameter takes the value of $4.79 \text{ Å}/\sin 70^\circ$.

Electron Microscopy. Isothermal crystallizations carried out on 2-methyl-pentanediol solutions in the 130–170 °C range usually give sheaf aggregates composed of long multilayered crystals (Figure 5a). However, great proportions of ribbonlike lamellae (Figure 5b) usually coexist in the high-temperature crystallizations. These lamellae show rather regular lateral edges, and are several microns long and about 0.2 μm wide. Also note that crystals appear frequently folded over themselves due to their long dimensions, and that the

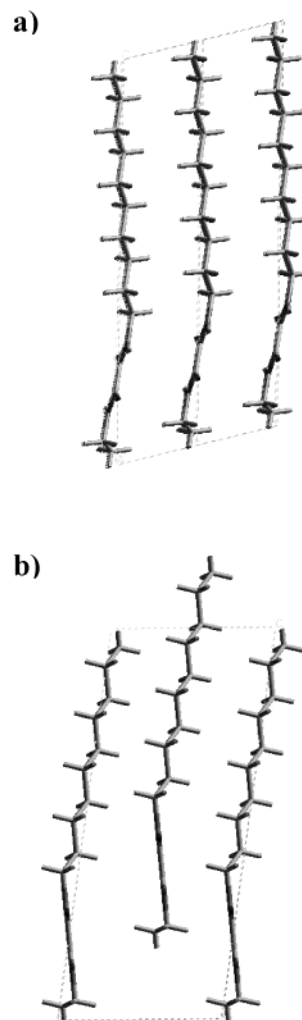


Figure 4. View along the a crystallographic axis of three hydrogen-bonded sheets corresponding to the postulated α structure with a chain axis shift of 1 Å (a) and a hypothetical β structure with recuperative shifts of 3.6 Å (b).

front edges (when they are not irregular due to some crystal cleavage) form an angle close to 64° (see arrows in Figure 5b) and similar to the expected γ crystallographic angle. A homogeneous thickness close to 60 Å can be deduced from the crystal shadows on electron micrographs and also from the low angle X-ray diffraction spacings of the mat of sedimented crystals (Figure 6). These are observed at 54 and 27 Å and correspond to the first and second lamellar orders, respectively. Meridional reflections at 14.1 and 7.0 Å are also found, suggesting that these crystals have the same crystalline structure detected in the powder patterns of samples coming directly from polymerization. Also note that the most intense reflection (indexed as 100) appears at 4.42 Å with an equatorial orientation, whereas the 010 and 110 planes give a broad reflection (3.70 Å) with a non equatorial orientation, a feature indicative of a unit cell with an α angle that clearly deviates from 90° .

Electron diffraction patterns were difficult to obtain, probably as a consequence of the expected tilting of the molecular chains with respect to the lamellar surfaces. However, it was possible to register a characteristic $hk0$ electron diffraction pattern from accidentally tilted samples. Note that the 100, 010, and 110 reflections are the most intense (Figure 7, Table 1). The 210 reflections are weaker and appear oriented along the long crystal

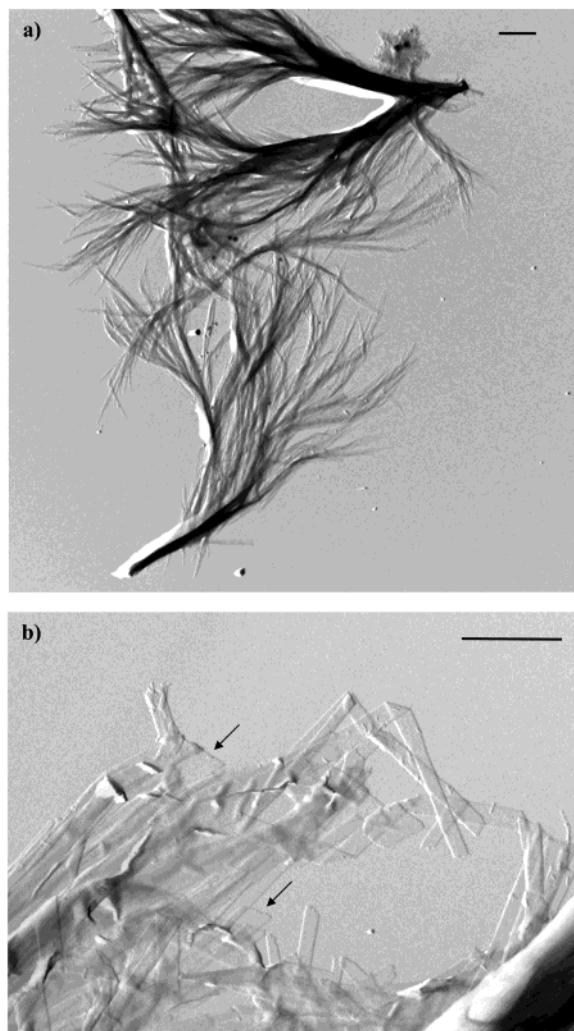


Figure 5. Electron micrographs corresponding to long sheaves (a) and ribbonlike crystals (b) obtained from nylon 12 2 crystallized on 2-methyl-2,4-pentandiol at 165 °C. Scale bars: 1 μm .

axis, indicating that hydrogen bonds are established along this direction, a fact that explains, as usual in polyamides, the high aspect ratio of the crystals.

The reduced crystal thickness, the molecular weight of the sample, and the electron diffraction data demonstrated that molecular chains are folded within the lamellar crystals. Polyethylene decoration of both sheaves and ribbonlike crystals (Figure 8) shows a regular folding surface. The decoration rods appear perpendicularly oriented to the long faces of the crystals, that is, along the hydrogen-bonding direction, suggesting a molecular folding habit parallel to the long dimension of the crystals.

Energy Calculations for Nylon 12 2. The packing energy of nylon 12 2 was calculated with the CERIU² program assuming different progressive shifts along the chain axis direction between the hydrogen-bonded sheets (Figure 9a). van der Waals, electrostatic and hydrogen-bonding terms were considered in the evaluation of the total energy. The low packing energy corresponds to shifts in the ± 4 Å range, the absolute minimum being obtained with a sheet displacement of + 1 Å. This value corresponds to an α angle of 75°, in agreement with the experimental evidence from X-ray fiber diffraction data. A second minimum close to the characterized two to

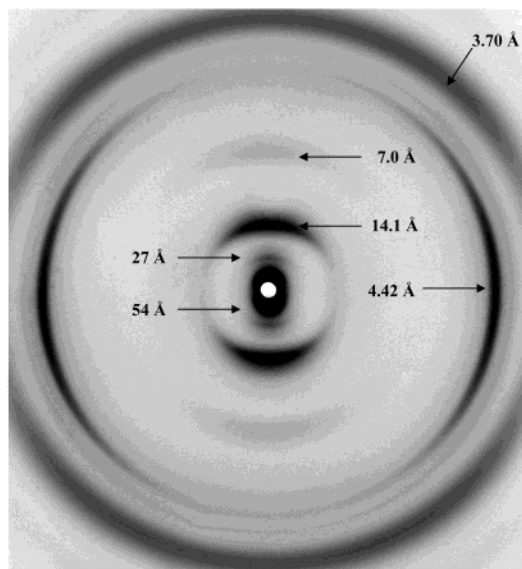


Figure 6. X-ray diffraction pattern of a mat of sedimented crystals obtained from isothermal crystallization on 2-methyl-2,4-pentandiol at 165 °C.

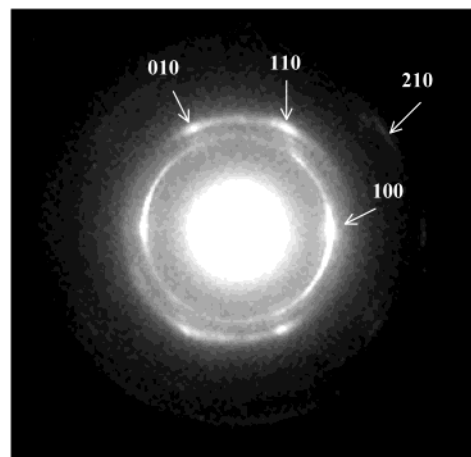


Figure 7. Single-crystal electron diffraction pattern of nylon 12 2. The 210 reflection is oriented along the crystal grown direction, indicating that hydrogen bonds run parallel to this direction.

three bond shift (+ 2.95 Å) can also be observed, but note that it is unstabilized by approximately a 2.4 kcal/mol of residue. We believe that this second minimum corresponds to the structure found in solution crystallized samples. A unit cell of parameters $a = 4.90$ Å, $b = 5.38$ Å, $c = 19.2$ Å, $\alpha = 48^\circ$, $\beta = 78^\circ$, and $\gamma = 65^\circ$ is proposed, taking into account the X-ray and electron diffraction data. In this case, the calculated shift corresponds to 3.6 Å. This value is slightly higher than that obtained from theoretical calculations but is in good agreement with the characteristic displacement found in the α -form of polyamides.

Figure 9b also shows the energy profiles as a function of the displacement of successive sheets assuming the typical alternating stacking of the β form. In this case, the energy curves are symmetrical, and consequently displacements in the up and down directions are absolutely equivalent. The total energy curve also shows a well-defined minimum close to a 1 Å shift. It must be pointed out that in order to maintain the same high energy contribution for the hydrogen-bonding interactions, we kept the values of $a = 4.90$ Å and $\beta = 78^\circ$,

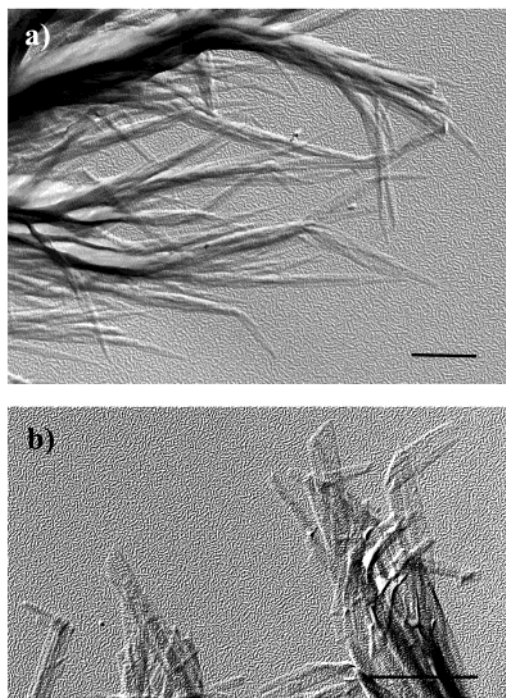


Figure 8. Polyethylene decoration of nylon 12 2 single crystals. Decorating rods appear frequently perpendicularly oriented to the long crystal edges. Scale bars: 1 μm .

even though they are not in agreement with the experimental cc^* angle of 20° . A difference of 0.3 kcal/mol of residue favors progressive sheet stacking.

PCSP calculations were also performed on nylon 12 2. The results obtained from these calculations can be summarized as follows. Staggered sheet packing was less stable than progressive packing by almost 1.6 kcal/mol of residue. Two minima at displacements of +0.92 and -4.47 Å were detected for the progressive model, the latter being 0.2 kcal/mol of residue more stable than the former. A symmetric energy profile was obtained for the staggered structure, the minima being located at ± 0.45 Å. A comparison between the results provided by both the CERIUS² and PCSP methods is displayed in Table 3. As can be seen, the two methods stabilize the progressive model with respect to the staggered one. However, some discrepancies related to the position and the relative stability of the minima were found between such two computational strategies. This was an expected result because the PCSP method uses a united atom approach for methylene groups, which has been reported to provide an unsatisfactory description of molecular systems with long polymethylene segments.^{19,20} Thus, although the united atom parametrization implemented in PCSP was very useful to study polyamides containing short aliphatic segments,^{21,22} the experimental data of nylon 12 2 have been poorly reproduced by this method.

Energy Calculations for Nylon 6 2. For the sake of completeness, the energy profiles of nylons 6 2 were also computed using both the CERIUS² and PCSP methodologies. Calculations were carried out assuming the model reported by Tadokoro et al.⁴ Thus, the energy terms were calculated assuming the parameters of $a = 5.15$ Å, c (fiber axis) = 12.39 Å, and $\beta = 73.5^\circ$. The α angle defines the sheet displacement and was consequently varied; the remaining b and γ parameters were selected in order to maintain the same chain axis projected unit cell (d_{100} , d_{010} , and d_{110} spacings). As

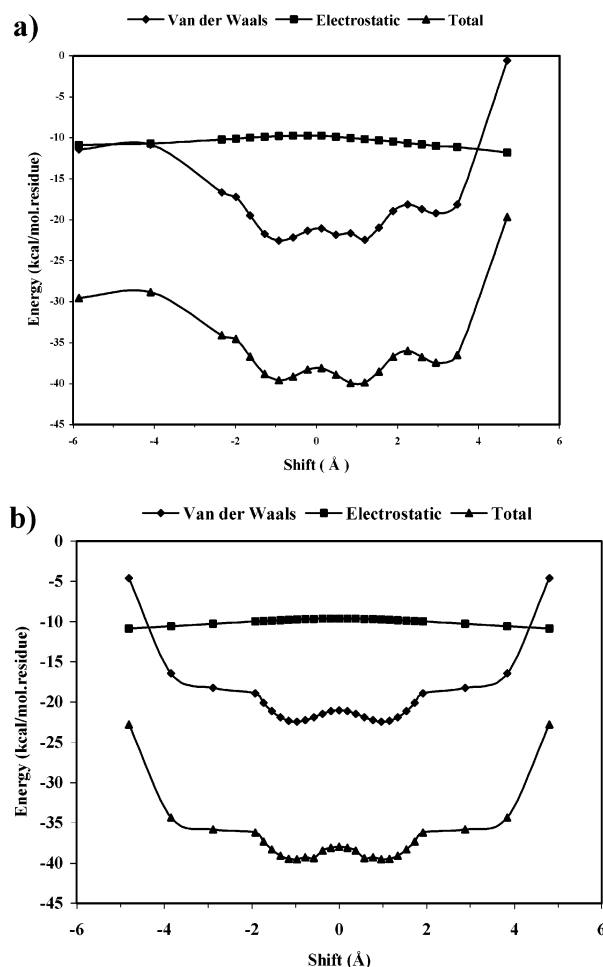


Figure 9. Energy profiles obtained with the crystal packer modulus of the CERIUS² program for nylon 12 2. Total energy and van der Waals and electrostatic contributions are plotted against the chain axis shift between consecutive sheets. Both the progressive arrangement of the α -structure (a) and the staggered disposition of the β form are represented (b). Only shifts in the -6 to $+6$ Å range are plotted due to the high energy values obtained for higher shifts.

Table 2. Measured and Calculated Spacings for X-ray and Electron Diffraction Patterns for Solution-Crystallized Samples of Nylon 12 2

| index | d_{calcd}^a (Å) | d_{measd}^b (Å) | |
|--------------------|--------------------------|----------------------------|---|
| | | mat of sedimented crystals | single-crystal electron diffraction pattern |
| 1st lamellar order | | 54 vs M | |
| 2nd lamellar order | | 27 m M | |
| 001 | 14.2 | 14.1 vs M | |
| 002 | 7.1 | 7.0 m M | |
| 100 | 4.39 | 4.42 vs E | 4.42 vs |
| 101, 111 | 4.09, 4.06 | 4.10 m E | |
| 010 | 3.68 | }3.70 s off E | 3.69 s |
| 110 | 3.60 | | 3.60 s |
| 111, 10 $\bar{1}$ | 3.11, 3.10 | 3.12 m | |
| 1 $\bar{1}$ 0 | 2.38 | | 2.40 m |
| 210 | 2.34 | | 2.33 m |
| 200 | 2.21 | | 2.21 m |

^a On the basis of a triclinic unit cell with $a = 4.90$ Å, $b = 5.38$, $c = 19.2$ Å, $\alpha = 48^\circ$, $\beta = 78^\circ$, and $\gamma = 65^\circ$. ^b Abbreviations denote relative intensities or orientation: vs, very strong; s, strong; m, medium; M, meridional; E, equatorial, off E, off equatorial.

indicated in the previous paper,⁴ the c parameter corresponds to a fully extended molecular chain, and therefore all torsional angles were fixed at 180° .

Table 3. Energy Minima Found for the Progressive and Alternate Models of Nylons 12 2 and 6 2 by Using the CERIUS² and PCSP Programs

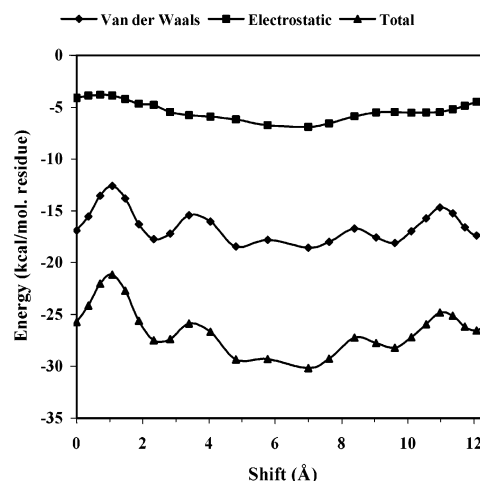
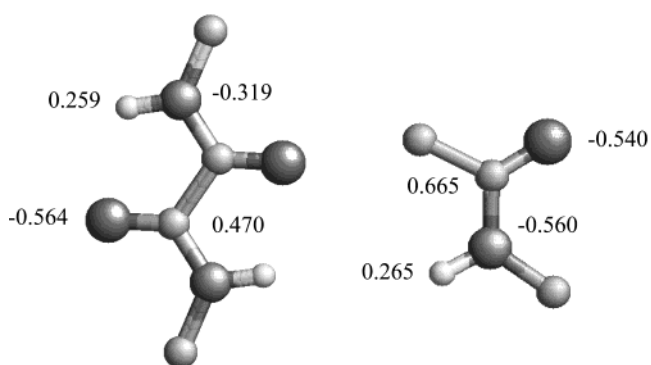
| nylon | method | model | displacement (Å) | ΔE (kcal/mol of residue) |
|-------|---------------------|--------------------------|------------------|----------------------------------|
| 12 2 | CERIUS ² | progressive (α) | + 1.00 | 0.0 |
| | | | - 1.00 | 0.4 |
| | | | + 2.95 | 2.4 |
| | PCSP | staggered (β) | \pm 1.00 | 0.3 |
| | | | + 0.92 | 0.2 |
| | | | + 5.30 | 0.5 |
| 6 2 | CERIUS ² | staggered (β) | - 4.47 | 0.0 |
| | | | \pm 0.45 | 1.6 |
| | | | + 7.00 | 0.0 |
| | | progressive (α) | + 4.81 | 0.8 |
| | | | + 9.61 | 1.9 |
| | | | + 2.40 | 2.6 |
| | PCSP | progressive (α) | + 12.09 | 3.6 |
| | | | + 6.92 | 0.0 |
| | | | + 4.82 | 0.1 |
| | | | + 9.97 | 0.4 |
| | | | + 3.00 | 1.1 |
| | | | + 11.95 | 2.3 |

Figure 10 shows the energy profile derived from CERIUS² calculations for the progressive model. The low methylene content of nylon 62 enhances the electrostatic contribution. Now the absolute energy minimum is observed for a shift between consecutive sheets of +7 Å, which is very close to a $d/2$ displacement. Moreover, four additional local minima with higher energies are also detected in the profile. The small size of the aliphatic segment allows a good description of nylon 62 using a united atom approximation. As a result, the energy profile provided by PCSP calculations almost matches that derived from CERIUS², the global minimum being also found at a displacement of $\sim d/2$. A more detailed comparison between the results obtained by the two methods is provided in Table 2. In addition, sensitivity of these energy calculations to small variations in the lattice was checked by performing complementary calculations for intersheet distances of 5.15 ± 0.10 Å, which is the widest margin of error experimentally acceptable. It was observed that, although the absolute energies fluctuate, the relative stability between the different minima was not qualitatively affected (data not shown).

Note that nylon 6 2 is a peculiar case because progressive and staggered sheet stackings coincide. Thus, no difference between the two models exists at $d/2$. It is also remarkable that this value is in agreement with the calculated shift for the experimental unit cell ($b \cos \alpha = 6.4$ Å). Finally, a deviation from the sheet displacement of the conventional α -form of nylons is detected again. Hence, the sheet displacements proposed for nylons 6 6, 4 6, and 6 were of 3.0,⁵ 3.6,²³ and 3.0²⁴–4.0²⁵ methylene units, respectively. Such difference is probably due to electron charge distributions on the oxalamide and amide groups. Thus, the former concentrates a large amount of negative charge in the oxygen atoms of the CO–CO moiety, which originates strong repulsive interactions with neighboring oxalamide groups. This effect is less important for conventional nylons. This is illustrated in Figure 11, which compares atomic charge distribution on oxalamide and amide groups.

Conclusions

In this work, we have presented a structural study on the even polyoxalamide derived from 1,12-dodecanediamine. The most remarkable result is that two

**Figure 10.** Energy profiles obtained with the crystal packer modulus of the CERIUS^{2.0} program for nylon 6 2. Total energy and van der Waals and electrostatic contributions are plotted against a progressive chain axis shift between consecutive sheets.**Figure 11.** Atomic charge distribution for oxalamide and amide groups.

crystalline forms can be obtained. They both consist of a progressive stacking of hydrogen-bonded sheets, but differ in the value of the chain axis shift between consecutive sheets. One of them is similar to the conventional α -form of nylons, whereas in the second one this value is reduced to only 1 Å. Packing energy calculations indicate as the most stable the 1 Å shift structure. Oxalamide groups have a distinct electron charge distribution from amide groups, and consequently the most stable structures of polyoxalamides and conventional nylons correspond to different shifts. Energy calculations performed with the polyoxalamide derived from 1,6-hexanediamine agree with the previously reported experimental results, and again demonstrated the influence of the oxalamide group in the stabilization of structures with nonconventional sheet stacking.

Acknowledgment. This investigation was supported by a research grant from Comisión Interministerial de Ciencia y Tecnología (CICYT) (MAT2000-099). E.A. acknowledges financial support from the Ministerio de Educación y Ciencia of Spain. The authors are indebted to CESCA for supercomputation facilities.

References and Notes

- Bruch, S. D. *Ind. Eng. Chem., Prod. Res. Dev.* **1963**, 2, 119.
- Black, W. D.; Preston, J. In *Man-Made Fibers, Science and Technology*; Mark, H. F., Atlas, S. M., Cernia, E., Eds.; Interscience: New York, 1968; Vol. 2, p 417.

- (3) Xenopoulos, A.; Clark, E. S. In *Nylons Plastics Handbook*; Kohan, M. I., Ed.; Hanser Publishers: Munich, Germany, 1995; Chapter 5.
- (4) Chatani, Y.; Ueda, Y.; Tadokoro, H.; Deits, W.; Vogl, O. *Macromolecules* **1978**, *11*, 636.
- (5) Bunn, C. W.; Garner, E. V. *Proc. R. Soc. London* **1947**, *A189*, 39.
- (6) Franco, L.; Subirana, J. A.; Puiggali, J. *Macromolecules* **1998**, *31*, 3912.
- (7) Armelin, E.; Alemán, C.; Puiggali, J. *J. Org. Chem.* **2002**, *66*, 8076.
- (8) Gaymans, R. J.; Venkatraman, V. S. *J. Polym. Sci., Polym. Phys. Ed.* **1984**, *22*, 1373.
- (9) Shalaby, S. W.; Pearce, E. M.; Fredericks, R. J.; Turi, E. A. *J. Polym. Sci., Polym. Phys. Ed.* **1973**, *11*, 1.
- (10) Wittmann, J. C.; Lotz, B. *J. Polym. Sci., Polym. Phys. Ed.* **1985**, *23*, 205.
- (11) CERIUS²; Biosym Molecular Simulations Inc.: Burlington, MA.
- (12) León, S.; Navas, J. J.; Alemán, C. *Polymer* **1999**, *40*, 7351.
- (13) Mayo, S. L.; Olafson, B. D.; Goddard, W. A. *J. Phys. Chem.* **1990**, *94*, 8897.
- (14) Weiner, S. J.; Kodman, P. A.; Nguyen, D. T.; Cabe, D. A. *J. Comp. Chem.* **1986**, *7*, 230.
- (15) Alemán, C.; Luque, F. J.; Orozco, M. *J. Comput. Aided Mol. Des.* **1993**, *7*, 721.
- (16) Urpí, L.; Villaseñor, P.; Rodríguez-Galán, A.; Puiggali, J. *Macromol. Chem. Phys.* **2000**, *201*, 1726.
- (17) Bermúdez, M.; León, S.; Alemán, C.; Bou, J. J.; Muñoz-Guerra, S. *Macromol. Chem. Phys.* **1999**, *200*, 2065.
- (18) Dasgupta, S.; Hammond, B.; Goddard, W. A. *J. Am. Chem. Soc.* **1996**, *118*, 12291.
- (19) Donal, E. W. *J. Comput. Chem.* **1994**, *15*, 719.
- (20) Dinur, U.; Hagler, A. T. *J. Comput. Chem.* **1995**, *16*, 154.
- (21) Bermúdez, M.; León, S.; Alemán, C.; Muñoz-Guerra, S. *J. Polym. Sci.: Polym. Phys.* **2000**, *38*, 41.
- (22) Bermúdez, M.; León, S.; Alemán, C.; Muñoz-Guerra, S. *Polymer* **2000**, *41*, 8961.
- (23) Bermúdez, M.; León, S.; Alemán, C.; Muñoz-Guerra, S. *J. Polym. Sci., Part B: Polym. Phys.* **2000**, *38*, 41.
- (24) Holmes, D. R.; Bunn, C. W.; Smith, D. J. *J. Polym. Sci.* **1955**, *17*, 159.
- (25) León, S.; Alemán, C.; Muñoz-Guerra, S. *Macromolecules* **2000**, *33*, 5754.

MA020869X